Drivers of variability of *Calanus finmarchicus* in the Gulf of Maine: roles of internal production and external exchange

Rubao Ji[1*], Jeffrey A. Runge[2], Cabell S. Davis[1], Peter H. Wiebe[1]

1. Woods Hole Oceanographic Institution, Woods Hole, MA 02543, USA
2. University of Maine, Darling Marine Center, Walpole, ME 0457, USA

Submit to: ICES Journal of Marine Sciences

Date: July 12, 2021

Running head: Variability of *Calanus finmarchicus* in the Gulf of Maine

***Corresponding author:** Rubao Ji (rji@whoi.edu)

Abstract

The lipid-rich calanoid copepod, *Calanus finmarchicus*, plays a critical role in the Gulf of Maine pelagic food web. Despite numerous studies over the last several decades, a clear picture of variability patterns and links with key environmental drivers remains elusive. This study applies model-based scaling and sensitivity analyses to a regional plankton dataset collected over the last four decades (1977-2017). The focus is to describe the gulf-wide spatio-temporal patterns across three major basins, and to assess the relative roles of internal population dynamics and external exchanges. For the spring stock, there is strong synchrony of interannual variability among three basins. This variability is largely driven by internal population dynamics rather than external exchanges, and the internal population dynamics are more sensitive to the change of top-down mortality regime than the bottom-up forcings. For the fall stock, the synchrony among basins weakens, and the variability is influenced by both internal mortality and external dilution loss. There appears to be no direct connection between the spring stock with either the preceding or subsequent fall stock, suggesting seasonal or sub-seasonal scales of population variability and associated drivers. The results highlight seasonally varying drivers responsible for population variability, including previously less recognized top-down control.

Keywords: Gulf of Maine, *Calanus finmarchicus*, Abundance variability, Synchrony, Bottom-up, Top-down

Introduction

The lipid-rich calanoid copepod, *Calanus finmarchicus*, is an important component of the Gulf of Maine (GoM, Fig 1) ecosystem. It has long been recognized as a foundation species in the GoM pelagic food web, transferring primary production to higher trophic levels, including important fishery species and endangered top predators such as right whales (e.g., Bigelow, 1926; Runge *et al.*, 2015; Ji *et al.*, 2017; Record *et al.*, 2019). The GoM, near the southern margin of the *C. finmarchicus* biogeographic distribution, could be especially vulnerable to a fast-warming climate. A substantial decline or possible disappearance of *C. finmarchicus* in the GoM, as predicted by some bioclimate models (e.g., Reygondeau and Beaugrand, 2011; Villarino *et al.*, 2015), would have a major impact on the entire regional ecosystem.

The temporal and spatial pattern of *C. finmarchicus* in the GoM was first comprehensively described in a 500-page report nearly a century ago by Henry Bigelow (Bigelow, 1926), who postulated that the maintenance of the population in the Gulf is largely controlled by local production rather than immigration from upstream regions to the east. Bigelow's view was later supported by Alfred Redfield (Redfield, 1941) based on the analyses of additional data collected in the 1930s. Redfield (1941) suggested that the recirculation of the GoM water contributes to the maintenance of the breeding stock in the Gulf and allows the population to persist in a largely advective system. He further argued that the Scotian Shelf Water inflow from the upstream region (Fig. 1) could 'dilute' the Gulf population – and the dilution effect is sufficiently strong to cause significant population fluctuations from year to year. Related early studies by Fish and Johnson (1937) and Mullin (1963) also conclude the Gulf is a largely closed system.

Those early views from pioneer oceanographers are remarkably insightful, yet they are undoubtedly constrained by the amount of data available at the time. For instance, their work did not recognize diapause in deep basins as an important life-history strategy in the GoM. Consequently, a full evaluation of the patterns and drivers of the population variability is missing. Since the Bigelow report, a large amount of data has become available from multiple regional plankton survey programs, particularly over the past five decades. The core question that has been debated over the years remains similar to what Bigelow and Redfield initially posed: is the variability in abundance driven by change in the biologically-driven population growth within the Gulf of Maine or by physically driven exchange with outside waters? This question was also coined as the predominance of production vs. supply in driving the variability (Greene *et al.*, 2004; Pershing *et al.*, 2009). It leads to follow-up questions: 1) If internal growth dominates, what are the relative roles of bottom-up or top-down control? 2) If external exchange dominates, does it supply or dilute the GoM population? Is the external exchange mainly along-shelf or at depth in the Northeast Channel (see Fig. 1 for a conceptual diagram)? 3) How do the controls vary over different seasons?

The above questions are seemingly simple but have proven to be challenging to answer. There are many reasons that contributed to this dilemma. At the data level, there is high uncertainty in the zooplankton measurements due to their high spatial patchiness (Mackas *et al.*, 1985;

Martin, 2003; Young *et al.*, 2009). A slight shift of sampling location or time could lead to a significant difference in observed abundance (notice that a time shift has a similar effect of location shift if sampling is not Lagrangian). This patchiness-induced representation error alone could induce uncertainty in assessing the general spatio-temporal pattern of variability, compromising the effort of identifying responsible environmental drivers. Long term observations with high spatial and temporal resolution could reduce some of the representation errors, although it would be logistically challenging. Like many other biological oceanography problems, in addition to the measurement uncertainty issue, there is also the challenge of identifying underlying mechanisms linking environmental drivers and zooplankton population dynamics. This challenge is especially pronounced when multiple nonlinearly interacting drivers are responsible for population variability. For instance, temperature can affect zooplankton populations via bioenergetic and reproductive rates, while also affecting prey availability (bottom-up) and predation pressure (top-down). Consequently, it is often difficult to establish a straightforward causal relationship between temperature and population variability, thus compromising population forecasting efforts.

Correlation analyses have been commonly used to study the association of *C. finmarchicus* variability with broad-scale climate forcing such as the North Atlantic Oscillation (NAO) (e.g., Conversi *et al.*, 2001; Licandro *et al.*, 2001; Greene and Pershing, 2003; MERCINA 2001, 2003, and 2004; Piontkovski *et al.*, 2006). Although the relationship is not necessarily causal, it can help generate hypotheses of potentially causal mechanistic links. For instance, through time-lagged regression analyses, NAO-forced changes in ocean circulation patterns and associated changes in external supply of *C. finmarchicus*, were proposed as the key drivers of Gulf of Maine population variability (MERCINA, 2004 and all the MERCINA-related references herein). This type of analysis provided a valuable theoretical framework to integrate a vast amount of physical and biological data and to test the proposed hypothesis. On the other hand, it is possible that the NAO could affect *C. finmarchicus* through multiple mechanistic pathways, such as the bottom-up pathway (hydrography → timing and magnitude of primary production →*C. finmarchicus* growth and reproduction) or the top-down pathway (hydrography → predator abundance and composition → predation loss of *C. finmarchicus*). Also, linking a large-scale index like the NAO can be difficult given location- and season-specific variabilities. It is thus reasonable to emphasize that, with results from correlation analyses alone, the underlying mechanisms remain elusive.

In this study, we take a step further and use a combined statistical analysis and process modeling approach, with a focus on patterns and dynamics overlooked in previous studies. Specifically, we examine the spatial synchrony patterns and responsible drivers across three major basins of the Gulf (see Fig. 1 for the locations) during both spring and fall seasons. Our approach is guided by a concept similar to Moran's (1953) theorem, which states that the synchrony of spatially separated populations results from synchrony of environmental drivers. Conversely, unsynchronized populations are likely driven by spatially unsynchronized environmental factors (either the same or different factors). Our approach is different from most of the previous studies, in which data were often aggregated into coarse spatio-temporal scales (e.g., a time series of the annual mean over the entire GoM), thus losing important dynamical information critical for revealing drivers responsible for the observed location- and season-specific variability. We also rely on a simple process-based population model for scaling analysis and sensitivity test. This approach allows us to gauge the importance of each term regulating population growth and the relevance of environmental indicators associated with fluctuations of internal dynamics (bottom-up and top-down) vs. exchanges with outside waters.

Materials and Methods

We use a combined data analysis and process modeling approach in this study. First, we process 41-year (1977-2017) survey data to describe season- and basin-specific anomalies of *C. finmarchicus* abundance in the GoM, and assess their temporal and spatial connections. Second, we conduct scaling analysis and sensitivity test based on a simple population model to better understand the underlying dynamics and provide a first-order deduction of potential drivers responsible for the observed variability.

Data analysis

This study relies mostly on the plankton survey data collected during the Marine Monitoring Assessment and Prediction (MARMAP, 1977 to 1987) and the subsequent Ecosystem Monitoring (EcoMon, 1988 to present) programs conducted by the U.S. NOAA Northeast Fisheries Science Center. The survey covers the Northeast US continental shelf and was conducted at approximately two-month intervals throughout the year (see Sherman, 1980; Meise and O'Reilly, 1996 and Kane, 2007 for program details and survey protocols). Plankton samples were collected at standard or randomly selected stations spaced approximately 8–35km apart with a 61-cm bongo net (333 µm mesh size) towed from a maximum depth of 200 m (or 5 m above the bottom for sites with bottom depths < 200 m) to the surface. The random strata design of sampling location selection is for minimizing spatial bias. The bimonthly to seasonal sampling frequency is relatively low, especially during the seasons when population size fluctuates strongly, and could lead to temporal sampling bias due to the so-called temporal aliasing problem. Moreover, survey cruises cannot cover a specific region synoptically or at exactly the same time each year, making it difficult for direct comparisons of abundance levels among different years. To minimize the potential sampling bias, we use an approach similar to the one developed by Kane (2007) to estimate interannual variability from 1977 to 2017. First, all the data points are pooled for three basins, including the Wilkinson Basin (WB), Jordon Basin (JB) and Georges Basin (GB) (see Fig. 1 for locations). It is worth noting that the 333 µm mesh net used by the MARMAP/EcoMon plankton survey program caught quantitatively the individuals with later copepodid stages (C3 and later) of *C. finmarchicus* efficiently, but significantly under-sampled the younger copepodid stages and likely also nauplii (see Anderson & Warren, 1991 for quantitative comparisons). Therefore, the variability patterns computed from this dataset largely comprise *C. finmarchicus* at older stages. The observed abundances are $\log_{10}$-transformed, and the average annual cycle of abundance is computed by spline-fitting the time-series of climatological monthly mean abundances (estimated from monthly binned abundances for each basin). This method generates the expected climatological abundance on any day of the year. Second, survey means then are subtracted from each original dataset to create anomalies, which can be binned and averaged for each season to produce a season-specific and basin-specific anomaly time series over the entire 41 years. Note also that the anomaly computed for each data point (before seasonal binning) has no detectable correlation with the sampling date (see Supplementary Material), suggesting that there is no systematic bias due to the difference in sampling dates across different years. Finally, conventional Pearson correlation analyses are conducted for time series among different basins in spring and fall seasons to assess spatial synchrony and also between spring and fall seasons (either spring and subsequent fall, or spring and preceding fall) to detect potential cross-season connections. Since autocorrelation in time series could potentially complicate statistical inference in correlation analyses, we compute the autocorrelation function (ACF) to detect the significance of autocorrelation at different time lags. No autocorrelation within reasonable time lags is detected in almost all time series based on our ACF calculation (see Supplementary Material). Thus results from the correlation analyses are not compromised by autocorrelation.

Modeling analysis

Following an approach developed by Aksnes & Blindheim (1996), the change of population size (N) over time (t) within a defined domain (e.g., the whole GoM, or individual basins within) can be described as:

$$dN/dt = rN + \varphi(N_b - N), \tag{1}$$

where r is the intrinsic population growth rate (birth minus death); N_b is the population size outside of the defined domain boundary, and here it is assumed to be proportional to N with a constant of k; φ represents the flushing rate, and is estimated as the inverse of flushing time T_f. Eq. (1) can be re-arranged as:

$$dN/dt = \left(r + {}^{(k-1)}/{}_{T_f}\right)N, \tag{2}$$

The term $\left(r + {}^{(k-1)}/{}_{T_f}\right)$ in Eq. (2) is equivalent to the per-capita growth rate (u), which can also be estimated from the observed change of population size from N_{t_1} at the time t_1 to N_{t_2} at the time t_2, using the exponential growth function:

$$u = \frac{\ln\left({}^{N_{t_2}}/{}_{N_{t_1}}\right)}{t_2 - t_1}\,. \tag{3}$$

We define $x = {}^{(k-1)}/{}_{T_f}$ as the physical exchange rate. Suppose the per-capita growth rate (u) and exchange rate (x) can be estimated, we can then assess the relative importance of intrinsic biological growth vs physical exchange by estimating the order of magnitude for each term. If the resulting scaling factor $s = u/x \gg 1$, then the intrinsic biological growth term dominates. Whereas if $s \sim 1$, the relative importance of intrinsic growth and external exchange is comparable.

The approximate mean values for u are estimated for both winter-spring growth season (positive growth) and summer-fall diapause season (negative growth) based on the climatological time series data. The average flushing time ($T_f \approx 30$ days) for basins during the winter-spring time period is estimated as the e-folding time for the decline of particles that remained in each basin after being released from the surface 50 meters and tracked using a Lagrangian approach as described in Ji et al. (2017). During the summer-fall time period, the focus is on the diapausing stock; therefore, the flushing time of deep water (> 100 m) is estimated instead. The tracking results from Johnson et al. (2006) suggested that the flushing time is in the order of 150~200 days, with a longer flushing time for WB and shorter for GB. The flushing time of surface water in the entire GoM is estimated to be at least 200 days based on the surface water volume flux (~$13*10^{12}$ m^3 yr^{-1}) and the volume of GoM surface 50 m water ($8*10^{12}$ m^3) (Smith et al., 2001). The above-mentioned values used in the scaling analysis are summarized in Table 1.

To diagnose the bottom-up and top-down controls, the intrinsic growth rate (r) can be estimated with the net reproductive rate (R_0) and average generation time (T_g) following Kiørboe and Sabatini, (1994):

$$r = {}^{ln(R_0)}/{}_{T_g}, \tag{4}$$

where R_0 can be calculated based on egg production rate (m), egg mortality rate (β_e), post-hatching mortality rate (β), egg hatching time (T_e) and total development time from egg to adult (D) using Eq. 5:

$$R_0 = \left({}^{m}/{}_{\beta}\right) e^{-(\beta_e - \beta)T_e - \beta D}, \tag{5}$$

and T_g can be estimated using Eq. 6:

$$T_g = \left(D + {}^{1}/{}_{\beta}\right). \tag{6}$$

The Eq. 2 now can be solved by substituting the r term using Eq. 4, such that the population size at time t (N_t) can be estimated if the initial population size (N_0) is known. This will allow us to test the sensitivity of N_t to the model parameters reflect bottom-up processes (e.g., m, T_e, and D, which are affected by food and temperature), top-down controls (e.g., β_e, β, which are affected by predation pressure), as well as external changes (e.g., T_f and k). For the sensitivity test purpose, the initial population size (N_0) can be scaled by an average value, so the normalized value (N_0^*) is dimensionless and varies around 1. The ranges of the above-mentioned parameters are listed in Table 2, along with the references from which the ranges are inferred. It is worth noting that the post-hatching mortality rate (β) varies beyond the range listed here, so the actual sensitivity to β could be higher than our estimation.

A global sensitivity analysis (GSA) of N_t to changes in parameter values within the range specified in Table 2 is conducted using a Matlab toolbox called SAFE (Sensitivity Analysis for Everybody) (http://bristol.ac.uk/cabot/resources/safe-toolbox/) developed by Pianosi et al. (2015), with a focus on the winter-spring population growth season. A GSA allows the evaluation of sensitivity over the full parameter space, and is different from the so-called local sensitivity analysis, which only allows changes around specific parameter values. Multiple GSA methods were available in the SAFE toolbox. In this study, we selected the Elementary Effect Test (EET) method (Morris, 1991), which estimates the mean of partial derivatives (Elementary Effect, EE) between model output and each randomly perturbed parameter. A higher mean EE indicates higher sensitivity. The standard deviation of EEs can also be calculated to assess the interaction between the target parameter and other parameters. A confidence bound can be estimated for the mean and the standard deviation of EEs via bootstrapping (Pianosi *et al.*, 2016).

Results

Spatio-temporal variability patterns

Climatologically, the GoM *C. finmarchicus* abundance has similar seasonality across the three major basins, with low abundances in winter months (February and March) and peaks in the spring months (mainly in May and June), before slowly declining during the summer and fall months (see Fig. 2, gray curves in the left panel). The wide spread of abundances around the climatological mean also suggests a strong variability, often with 1-2 orders of magnitude of deviation from the mean. This variability can also be seen from the anomaly plots from different seasons in Fig. 2 (right panel).

The correlation analysis for the spring season anomalies shows significant correlations among three basins (Fig. 3, left panel), with correlation coefficients (r) above 0.36 and p-values less than 0.05. On the contrary, significant correlation of the fall season anomalies only exist between WB and JB ($r = 0.73$, $p < 0.01$), but not with GB ($p > 0.05$) (Fig. 3, right panel). The results indicate location- and season-specific synchrony patterns in terms of the interannual variability of *C. finmarchicus* abundance across the GoM basins.

From the coefficient analyses between spring and fall seasons (Table 3), it is clear that there is no positive seasonal ‘carry-over’ effect for most of the basin populations, either from spring to subsequent fall, or from fall to the subsequent spring. The only exception is within GB, where the spring anomaly is significantly and positively correlated with the fall anomaly. For all the other cases, either within or across basins, no significant positive correlation exists. In other words, a large diapausing population during fall in one basin does not necessarily lead to a large spring population in the same basin or other basins. A similar disconnect is found from spring to the subsequent fall. Mathematically, it implies that the population sizes in spring or fall are not controlled by their initial condition. The table 3 also shows cases with significant but negative correlations. One is for spring vs subsequent fall within JB as well as between WB and JB, and the other is for spring vs. preceding fall within JB. Those negative correlations are difficult to interpret, and could be related to predator-prey interactions. More data would be needed to develop a plausible explanation. Nevertheless, the key finding from this analysis is the lack of significant positive correlation across seasons.

Scaling analysis

The analysis is based on the Eq. 2 and 3 with the parameters listed in Table 1. During the winter-spring growing season, the increase of population size ($^{N_{t_2}}/_{N_{t_1}}$) is nearly one order of magnitude at either the basin- or the GoM-scale over two months. This increase is equivalent to a per-capita population growth rate of 0.038 day^{-1}. Two external exchange scenarios are considered at both the local basin- and GoM-scales. For the low-exchange scenario at the local basin-scale, the ratio of boundary to internal population size is lower, and the flushing time is longer than the high-exchange scenario. Consequently, in the low-exchange scenario ($k = 1.2$, and $T_f = 40 \text{ days}$), the per-capita growth rate is nearly one order of magnitude higher than the exchange rate, suggesting a significant contribution of the intrinsic growth rate ($r = u - x$) in regulating the net population growth. For the high exchange scenario ($k = 2.0$, and $T_f = 20$ days), the contribution of the intrinsic growth has a similar order of magnitude as the external exchange. At the scale of entire GoM, it is clear that intrinsic growth is much more important than the external exchange since the exchange rates are low under both exchange scenarios. It is worth noting that Table 1 only listed the case with $k > 1$ (abundance is higher at the boundary than inside of the domain). A similar scaling analysis can be done for cases with $k < 1$, and the results are similar to the cases with $k > 1$, although the external exchange dilutes the internal population.

During the summer and fall seasons, the population resides mainly in the deep local basins as diapausers (composed mainly of copepodid stage 5, C5). Its abundance declines gradually by nearly 1/3 over a ~200 day time period, resulting in a negative per-capita growth rate of -0.006 day^{-1}. This is within the same order of magnitude as the external exchange rate, either at a low- or high- exchange scenario.

Sensitivity analysis

The global sensitivity analysis results are shown in Fig. 4, with the model-computed population size after a 60-day integration (mimicking the winter-spring growing time window) most sensitive to the post-hatching mortality rate (β) at either the basin- or the GoM-scale, followed by the development time (*D*). The model is much less sensitive to the other parameters, including the initial population size (N_0) and other life-history parameters. The intensity of interaction (standard deviation of EEs) follows the same pattern as the sensitivity (mean of EEs), with the β and *D* ranked top 1 and 2, respectively. This finding suggests that the sensitivity of a highly sensitive parameter is also significantly influenced by the other parameters and vice versa. For instance, the sensitivity of β could fluctuate much more than the other parameters at different parameter spaces.

Discussion

Internal growth (production) vs. external change (supply)

Our scaling results suggest that internal growth is the key source of population variability during the winter-spring growing season at the GoM scale, and likely also at the local basin-scale. Given the lack of influence from the preceding fall population (Table 3), it is reasonable to argue that the local vital rates, rather than the seeding population size (initial condition), play a more important role. This is also supported by our sensitivity analysis for the population growth during the winter-spring transition time. Other supporting evidence emerges from the spatial synchrony pattern. The mean seasonality of *C. finmarchicus* population across the three basins is synchronized to a large degree (Fig. 2, left panel), which would not have been possible if the population is propagated through advection since transport time among basins is on the order of 1-2 months. The cross-basin synchrony of the spring population at the interannual scale (Fig. 3, left panel) also suggests the importance of internal growth over external exchange as the interannual variability of external change is less likely synchronized across the three basins. Our results are in agreement with an early study by Mullin (1963), who suggested a limited influence of external exchange based on the body size difference between the “inside” eastern Gulf population and the “outside” slope population.

The situation is different for the variability of the fall population. Our scaling analysis suggests that internal and external processes could play a similarly important role. With a relatively faster flushing regime and closer proximity to Slope Water, GB is likely to be more susceptible to exchange with the Slope Water, causing the asynchrony between the GB and the other two basins (Fig. 3, right panel). Deep water entering the inner basins carries a mixture of GB and Slope Water populations, reducing the exchange loss of the inner basins due to the weakened abundance gradient (k) with their surrounding deep water. Instead, both WB and JB populations could share other similar drivers, including population supplies from the coastal region connected to the upstream Scotian Shelf (Ji et al., 2017) and/or stronger top-down controls through mortality loss. This may result in strong synchrony between WB and JB population anomaly (Fig. 3, right panel). A 'powershift' between the internal and external processes could occur in different basins and from year to year, making it difficult to establish a generic link between the population variability and a single environmental driver. Record et al. (2019) found a significant correlation between the *C. finmarchicus* abundance and bottom temperature in the JB during the diapause seasons after 2004. However, this relationship cannot be detected in the earlier decades nor in other basins, highlighting the need to consider multiple drivers when assessing population variability.

Previous studies by the MERCINA group (MERCINA, 2004 and all the MERCINA-related references herein), suggested that the NAO-regulated Slope Water intrusion was the dominant driver of population variability at the GoM-scale. There are two major assumptions in this hypothesis. First, low NAO is associated with more intrusion of the Labrador Subarctic Slope

Water (LSSW) than the Warm Slope Water (WSW) into the GoM through the Northeast Channel. Second, the *C. finmarchicus* abundance in the WSW is higher than that in the LSSW. Both assumptions are debatable. First, new hydrographic data (Ecosystem Assessment Program, 2012) indicate that the regulation of NAO on Slope Water intrusion is less discernable since the early 2000s. Second, limited sampling data in the Slope Water region indicate that both WSW and LSSW carry a very low abundance of *C. finmarchicus* during summer and fall, especially at a depth conducive to Slope Water intrusion over the shallow sill (~230 m) in the Northeast Channel. The abundance in the WSW could in fact be lower than that in the LSSW. For example, Miller et al. (1991) observed no *C. finmarchicus* at depths shallower than 300 m in the Slope Water area south of New England (WSW proper), whereas Head and Pepin (2008) reported abundances less than 10 inds. m^{-3} in the LSSW proper. In either case, the Slope Water population abundance is on average more than one order of magnitude lower than the basin populations.

The intermingling of bottom-up and top-down controls

During the winter-spring transition time when the population grows exponentially, the post-hatching mortality, β, appears to be the most sensitive parameter, either at the local basin- or the whole GoM-scale (Fig. 4). Taken at face value, this result can be interpreted as indicating that top-down control is the dominant driver of population variability. However, the situation could be much more complicated due to the intermingling of the bottom-up and top-down controls (Fig. 5, left panel). This interplay is reflected in the high standard deviation of model sensitivity to the post-hatching mortality β, suggesting a strong interaction with bottom-up factors could cause high fluctuation of β in different environmental regimes.

Considering the scenario of food availability as a bottom-up forcing, both the development rate and fecundity of *C. finmarchicus* will increase as more food is available (Campbell *et al.*, 2001), allowing a shorter generation time and earlier ramp up of population size. This nutritional enhancement will help the population to achieve a higher peak due to shorter exposure to predation pressure and a mismatch with the peak predation pressure at a later date (Fig. 5, right panel). There is evidence that food availability to females for egg production has increased recently in WB in late winter (Feb-Mar), allowing for an earlier spring cohort (Runge *et al.*, 2015; Record *et al.*, 2019) subject to lower mortality rates. This concept is similar to the slow-growth-high-mortality hypothesis initially proposed for herbivorous insects (Feeny, 1976) and the growth-mortality hypothesis in fisheries oceanography (e.g., Anderson, 1988; Davis *et al.*, 1991).

The role of temperature is also not straightforward. On the one hand, warmer water can lead to an earlier growing season and also speed up development (equivalent to bottom-up effect), thus mitigating high predation pressure as the above growth-mortality hypothesis suggested. Higher temperature however can exacerbate food limitation in copepods (Vidal, 1980) and predators might also respond to a higher temperature by shifting their seasonality and increase their predation rate. Moreover, novel predators (such as jellyfish) could bloom in a warmer regime, causing a drastic decline in the population size.

During the summer-fall diapausing season, there is no bottom-up influence in terms of the food supply. Since the diapausing population resides deeper than 150 meters and predation risk from visual predators drops significantly (see an example from Huse and Fiksen, 2010), invertebrate predators, such as siphonophores, euphausiids, chaetognaths and *Paraeucheata* are likely the primary top-down driver. Observations using Video Plankton Recorder (VPR) and bioacoustics have shown the presence of those invertebrate predators in the deep basins of the GoM (Benfield *et al.*, 2003; Lavery *et al.*, 2007). However, if we consider the temperature-dependent consumption of lipid reserve in the diapausers as a bottom-up-equivalent forcing, then both bottom-up and top-down controls are present for the diapausing population. In this case, a warmer bottom temperature will result in the consumption of the lipid energy reserve faster, forcing the individuals to exit the diapausing phase earlier (Saumweber and Durbin, 2006; Pierson *et al.*, 2013) and causing a higher mortality rate.

Conclusions

The scale- and season-dependent variability of *C. finmarchicus* population revealed from a long-term survey dataset provided a unique opportunity to diagnose responsible environmental drivers. Our scaling analysis suggests a dominant role of internal population growth in driving the spring population variability when compared with the external exchange process, while both could have a similar impact on fall population variability. The spring population is most sensitive to the top-down component of the internal growth term (represented as the post-hatching mortality rate). However, this top-down control is affected by the bottom-upregulated timing and rate of population growth. Our process-based analysis of population dynamics could help guide future observation and modeling efforts for a better future projection of *C. finmarchicus* in the Gulf of Maine.

Data availability

The *Calanus finmarchicus* abundance data collected from the MARMAP/EcoMon survey program are publicly accessible at the NOAA National Centers for Environmental Information site (https://www.ncei.noaa.gov/archive/accession/0187513) [See reference: Northeast Fisheries Science Center (NMFS/NEFSC), 2019].

Acknowledgement

This work was supported by the US MBON Gulf of Maine project to NERACOOS (NOPP award NA19NOS0120197 and BOEM-UMaine Cooperative Agreement M19AC00022), and the Northeast US Shelf Long Term Ecological Research (NES-LTER) project (NSF OCE-1655686). The MARMAP/EcoMon dataset was provided by the US National Marine Fisheries Service through D. Richardson and H. Walsh. We gratefully acknowledge the great efforts of numerous NEFSC managers, staff, and shipboard scientists and crew who collected plankton samples and managed the database over the last four and half decades. Most of the samples were sorted and identified at the Polish Plankton Sorting and Identification Center in Szczecin, Poland. We would also like to acknowledge three anonymous reviewers for their constructive comments. Finally, Dr. Steve Hay was a colleague with us for many years within the ICES Working Group for Zooplankton Ecology. Over the years we had many stimulating discussions with Dr. Hay about

Calanus finmarchicus and other zooplankton species and fisheries oceanography in general. We dedicate this paper to his memory. His presence will be missed by all of us.

References

Aksnes, D. L., and Blindheim, J. 1996. Circulation patterns in the North Atlantic and possible impact on population dynamics of Calanus finmarchicus. Ophelia, 44: 7–28.

Anderson, J. T. 1988. A review of size dependent survival during pre-recruit stages of fishes in relation to recruitment. Journal of Northwest Atlantic Fishery Science, 8: 12.

Anderson, J. T., and Warren, W. G. 1991. Comparison of catch rates among small and large Bongo sampler for *Calanus finmarchicus* copepodite stages. Canadian Journal of Fisheries and Aquatic Sciences. 48: 303-308.

Benfield, M., Lavery, A., Wiebe, P., Greene, C., Stanton, T., and Copley, N. 2003. Distributions of physonect siphonulae in the Gulf of Maine and their potential as important sources of acoustic scattering. Canadian Journal of Fisheries and Aquatic Sciences - CAN J FISHERIES AQUAT SCI, 60: 759–772.

Bigelow, H. B. 1926. Plankton of the offshore waters of the Gulf of Maine, 40: 1–509.

Campbell, R. G., Wagner, M. M., Teegarden, G. J., Boudreau, C. A., and Durbin, E. G. 2001. Growth and development rates of the copepod *Calanus finmarchicus* reared in the laboratory. Marine Ecology Progress Series, 221: 161–183.

Conversi, A., Piontkovski, S., and Hameed, S. 2001. Seasonal and interannual dynamics of Calanus finmarchicus in the Gulf of Maine (Northeastern US shelf) with reference to the

North Atlantic Oscillation. Deep Sea Research Part II: Topical Studies in Oceanography, 48: 519–530.

Davis, C., Flierl, G., Wiebe, P. H., and Franks, P. 1991. Micropatchiness, turbulence and recruitment in plankton. Journal of Marine Research, 49: 109–151.

Ecosystem Assessment Program. 2012. Ecosystem Status Report for the Northeast Shelf Large Marine Ecosystem - 2011. US Dept Commer, Northeast Fish Sci Cent Ref Doc. 12-07; 32 p. Available from: National Marine Fisheries Service, 166 Water Street, Woods Hole, MA 02543-1026, or online at http://www.nefsc.noaa.gov/nefsc/publications/.

Feeny, P. 1976. Plant Apparency and Chemical Defense. *In* Biochemical Interaction Between Plants and Insects, pp. 1–40. Ed. by J. W. Wallace and R. L. Mansell. Springer US, Boston, MA. https://doi.org/10.1007/978-1-4684-2646-5_1 (Accessed 7 February 2021).

Fish, C. J., and Johnson, M. W. 1937. The Biology of the Zooplankton Population in the Bay of Fundy and Gulf of Maine with Special Reference to Production and Distribution. Journal of the Biological Board of Canada, 3: 189–322.

Greene, C., Pershing, A., Monger, B., Benfield, M., Durbin, E., and Casas, M. 2004. Supply-Side Ecology and the Response of Zooplankton to Climate-Driven Changes in North Atlantic Ocean Circulation. Oceanography, 17: 60–71.

Greene, C. H., and Pershing, A. J. 2003. The flip-side of the North Atlantic Oscillation and modal shifts in slope-water circulation patterns. Limnology and Oceanography, 48: 319–322.

Head, E., and Pepin, P. 2008. Variations in overwintering depth distributions of *Calanus finmarchicus* in the slope waters of the NW Atlantic Continental Shelf and the Labrador Sea. Journal of Northwest Atlantic Fishery Science, 39: 49–69.

Huse, G., and Fiksen, Ø. 2010. Modelling encounter rates and distribution of mobile predators and prey. Progress in Oceanography, 84: 93–104.

Ji, R., Feng, Z., Jones, B. T., Thompson, C., Chen, C., Record, N. R., and Runge, J. A. 2017. Coastal amplification of supply and transport (CAST): a new hypothesis about the persistence of *Calanus finmarchicus* in the Gulf of Maine. ICES Journal of Marine Science, 74: 1865–1874.

Johnson, C., Pringle, J., and Chen, C. 2006. Transport and retention of dormant copepods in the Gulf of Maine. Deep Sea Research Part II: Topical Studies in Oceanography, 53: 2520–2536.

Kiørboe, T., and Sabatini, M. 1994. Reproductive and life cycle strategies in egg-carrying cyclopoid and free-spawning calanoid copepods. J. Plankton Res., 16: 1353–1366.

Lavery, A., Wiebe, P., Stanton, T., Lawson, G., Benfield, M., and Copley, N. 2007. Determining dominant scatterers of sound in mixed zooplankton populations. The Journal of the Acoustical Society of America, 122: 3304–26.

Licandro, P., Conversi, A., Ibanez, F., and Jossi, J. 2001. Time series analysis of interrupted long-term data set (1961-1991) of zooplankton abundance in Gulf of Maine (northern Atlantic, USA). Oceanologica Acta, 24: 453–466.

Mackas, D. L., Denman, K. L., and Abbott, M. R. 1985. Plankton patchiness: biology in the physical vernacular. Bulletin of Marine Science, 37: 652–674.

Martin, A. P. 2003. Phytoplankton patchiness: the role of lateral stirring and mixing. Progress in Oceanography, 57: 125–174.

Meise, C. J., and O'Reilly, J. E. 1996. Spatial and seasonal patterns in abundance and age-composition of *Calanus finmarchicus* in the Gulf of Maine and on Georges Bank: 1977-1987. Deep Sea Research Part II: Topical Studies in Oceanography, 43: 1473–1501.

MERCINA (Marine Ecosystem Responses to Climate in the North Atlantic). 2001. Oceanographic responses to climate in the northwest Atlantic. Oceanography, 14:76-82.

MERCINA (Marine Ecosystem Responses to Climate in the North Atlantic). 2003. Trans-Atlantic responses of *Calanus finmarchicus* populations to basin-scale forcing associated with the North Atlantic oscillation. Progress in Oceanography, 58:301-312.

MERCINA (Marine Ecosystem Responses to Climate in the North Atlantic). 2004. Supply-side ecology and the response of zooplankton to climate-driven changes in North Atlantic Ocean circulation. Oceanography, 17(3):60–71.

Miller, C. B., Cowles, T. J., Wiebe, P. H., Copley, N. J., and Grigg, H. 1991. Phenology in *Calanus finmarchicus*; hypotheses about control mechanisms. Marine ecology progress series. Oldendorf, 72: 79–91.

Moran, P. A. 1953. The statistical analysis of the Canadian lynx cycle. Australian Journal of Zoology, 1: 291–298. CSIRO.

Morris, M. D. 1991. Factorial sampling plans for preliminary computational experiments. Technometrics, 33: 161–174. Taylor & Francis.

Mullin, M. M. 1963. Comparative ecology of the genus *Calanus* in the Gulf of Maine. PhD thesis, Department of Biology, Harvard University.

Northeast Fisheries Science Center (NMFS/NEFSC). 2019. Zooplankton and ichthyoplankton abundance and distribution in the North Atlantic collected by the Ecosystem Monitoring

(EcoMon) Project from 1977-02-13 to 2017-11-16 (NCEI Accession 0187513). NOAA National Centers for Environmental Information. https://www.ncei.noaa.gov/archive/accession/0187513.

Pershing, A., Record, N., Monger, B., DE, P., and LA, W. 2009. Model-based estimates of *Calanus finmarchicus* abundance in the Gulf of Maine. Marine Ecology Progress Series, 378: 227–243.

Pianosi, F., Sarrazin, F., and Wagener, T. 2015. A Matlab toolbox for Global Sensitivity Analysis. Environmental Modelling & Software, 70: 80–85.

Pianosi, F., Beven, K., Freer, J., Hall, J. W., Rougier, J., Stephenson, D. B., and Wagener, T. 2016. Sensitivity analysis of environmental models: A systematic review with practical workflow. Environmental Modelling & Software, 79: 214–232.

Pierson, J. J., Batchelder, H., Saumweber, W., Leising, A., and Runge, J. 2013. The impact of increasing temperatures on dormancy duration in *Calanus finmarchicus*. Journal of Plankton Research, 35: 504–512.

Piontkovski, S. A., O'brien, T. D., Umani, S. F., Krupa, E. G., Stuge, T. S., Balymbetov, K. S., Grishaeva, O. V., *et al.* 2006. Zooplankton and the North Atlantic Oscillation: a basin-scale analysis. Journal of Plankton Research, 28: 1039–1046. Oxford Academic.

Record, N., Runge, J., Pendleton, D., Balch, W., Davies, K., Pershing, A., Johnson, C., *et al.* 2019. Rapid climate-driven circulation changes threaten conservation of endangered North Atlantic right whales. Oceanography, 32. https://tos.org/oceanography/article/rapid-climate-driven-circulation-changes-threaten-conservation-of-endangere (Accessed 23 May 2019).

Redfield, A. C. 1941. The effect of the circulation of water on the distribution of the Calanoid community in the Gulf of Maine. The Biological Bulletin, 80: 86–110.

Reygondeau, G., and Beaugrand, G. 2011. Future climate-driven shifts in distribution of *Calanus finmarchicus*. Global Change Biology, 17: 756–766.

Runge, J. A., Ji, R., Thompson, C. R. S., Record, N. R., Chen, C., Vandemark, D. C., Salisbury, J. E., *et al.* 2015. Persistence of *Calanus finmarchicus* in the western Gulf of Maine during recent extreme warming. Journal of Plankton Research, 37: 221–232.

Saumweber, W. J., and Durbin, E. G. 2006. Estimating potential diapause duration in *Calanus finmarchicus*. Deep Sea Research Part II: Topical Studies in Oceanography, 53: 2597–2617.

Sherman, K. 1980. MARMAP, a fisheries ecosystem study in the northwest Atlantic: fluctuations in ichthyoplankton-zooplankton components and their potential for impact on the system. Advanced Concepts in Ocean Measurements for Marine Biology. Belle W. Baruch Institute for Marine Biology and Coastal Research. University of South Carolina Press. Columbia, SC, 572.

Vidal, J. 1980. Physioecology of zooplankton. I. Effects of phytoplankton concentration, temperature, and body size on the growth rate of *Calanus pacificus* and *Pseudocalanus* sp. Marine Biology, 56: 111–134.

Villarino, E., Chust, G., Licandro, P., Butenschon, M., Ibaibarriaga, L., Larrañaga, A., and Irigoien, X. 2015. Modelling the future biogeography of North Atlantic zooplankton communities in response to climate change. Marine Ecology Progress Series, 531: 121–142.

Young, K. V., Dower, J. F., and Pepin, P. 2009. A hierarchical analysis of the spatial distribution of larval fish prey. Journal of Plankton Research, 31: 687–700.

Figure captions

Figure 1. **Left panel:** The Gulf of Maine bathymetry map, showing the locations of three basins, Wilkinson Basin, Jordan Basin and Georges Basin, in which high abundances of *Calanus finmarchicus* are often found diapausing over summer and fall. Scotian Shelf Water (SSW) enters from the right and Gulf of Maine surface water enters the New England Shelf to the left. Deep water exchange (red bi-direction arrow) occurs mainly through the Northeast Channel connecting the Georges Basin and the slope. **Right panel:** A conceptual illustration of the internal life cycle and external exchange of *C. finmarchicus* population in the Gulf of Maine. Bathymetry base map courtesy: Ed Roworth & Rich Signell from USGS, https://pubs.usgs.gov/of/1998/of98-801/bathy/images/gom5.jpg.

Figure 2. Left panel: Scatter plots of log-transformed *C. finmarchicus* abundance in three deep basins of the GoM, showing all data points at different year dates for all years from 1977 to 2017. The gray curve is the spline-fit of monthly binned and averaged abundances for each basin. **Right panel:** Season-specific anomalies of log-transformed *C. finmarchicus* abundance for all three basins from 1977 to 2017. The winter season includes January, February and March (JFM); the spring season includes April, May and June (AMJ); the summer season includes July, August and September (JAS); and the fall season includes October, November and December (OND). Sea text for the detail of anomaly calculation. WB: Wilkinson Basin (top panel); JB: Jordan Basin (middle panel); GB: Georges Basin (bottom panel)

Figure 3. Time series of *C. finmarchicus* abundance anomaly (log10-transformed, inds m^{-3}) in three deep basins of the GoM, showing significant correlation among three basins during spring months (l**eft panel**; AMJ: April, May and June), but only two basins (WB and JB) are correlated during fall months (**right panel**; OND: October, November and December). The correlation coefficients (*r*) and *p*-values are shown inside the plots. WB: Wilkinson Basin; JB: Jordan Basin; GB: Georges Basin.

Figure 4. Global sensitivity analysis for population growth to different parameters at the basin scale (**left panel**) or for the entire Gulf of Maine (**right panel**). The mean of EEs (Elementary Effects) in the x-axis represents the sensitivity for each parameter, and the standard deviation of EEs in the y-axis represents the interaction of a specific parameter with other parameters. A higher standard deviation of EEs suggests stronger interactions between the target parameter with the other parameters. The width and height of the rectangle surrounding each data point (as a black circle) represent the confidence bounds for the mean and standard deviation of EEs, respectively.

Figure 5. The intermingling of bottom-up and top-down controls. **Left panel** shows the how food and temperature could be linked to both bottom-up and top-down processes. Changes in food and temperature could affect development and fecundity directly. Changes in development duration and reproduction timing could affect the population's exposure to mortality loss, therefore indirectly affect top-down control. **Right panel** shows the concept of the growth-mortality hypothesis. In panel **A**, the population growth is overlapped with the increase of predation pressure, and the maximum population size is suppressed when compared with the scenario in panel **B**, showing that population has already reached a large size when the predation pressure peaks.

Table 1. The parameters and results for the scaling analyses based on Eq. (2) and (3). The analyses are conducted at two different spatial scales, one for the local basin-scale (e.g. WB, JB and GB), and the other for the whole GoM-scale. For the local basin-scale, two time periods are examined, covering the winter-spring population growth phase (a 60-day period starting from mid-March) and the summer-fall population declining phase (a 200-day period starting from the beginning of July). For the whole GoM-scale, only the winter-spring period is examined.

Scale (Season)	N_{t_2}/N_{t_1}	$t_2 - t_1$ (day)	u (day^{-1})	k	T_f (day)	x (day^{-1})	s ($= u/x$)
Basin-scale (winter-spring)	10	60	0.038	1.2	40	0.007	5.4*
				2.0	20	0.050	0.8
Basin-scale (summer-fall)	1/3	200	-0.006	0.1	150	-0.006	1.0
				0.6	200	-0.002	3.0
GoM-scale (winter-spring)	10	60	0.038	1.2	250	0.001	38.0*
				2.0	200	0.005	7.6*

* indicates u is one order of magnitude higher than x after rounding.

Table 2. Ranges of parameters used for the global sensitivity analysis. See text for the meaning of each variable.

Region	m (eggs day^{-1} ind^{-1})	β (day^{-1})	β_e (day^{-1})	D (day)	T_e (day)	T_f (day)	k	N_0^*
Basin	[20,100]	[0.05,0.3]	[0.5,1.0]	[30,60]	[1,3]	[20,40]	[0.5,2.0]	[0.3,3.0]
GOM	[20,100]	[0.05,0.3]	[0.5,1.0]	[30,60]	[1,3]	[100,200]	[0.5,2.0]	[0.3,3.0]
Reference	Runge et al. (2006)	Ohman et al. (2002)		Campbell et al. (2001)		This study		

Table 3. correlations between spring and fall (* means a statistically significant correlation at 95% significance level). The only significant positive correlation shown in bold.

Spring vs. subsequent fall

Fall Spring	JB	WB	GB
JB	-0.458*	-0.248	0.048
WB	-0.455*	-0.285	-0.002
GB	-0.243	0.093	**0.355***

Spring vs. preceding fall

Fall Spring	JB	WB	GB
JB	-0.484*	-0.197	-0.251
WB	-0.317	0.173	-0.283
GB	-0.171	-0.120	0.017

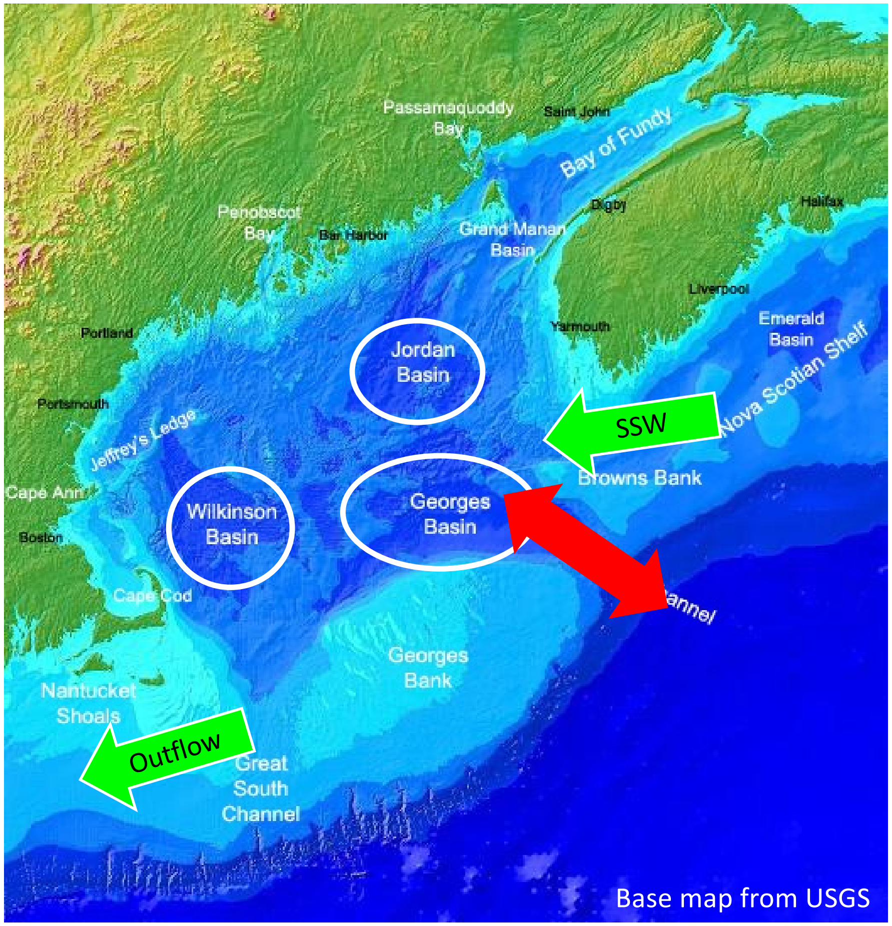
Passamaquoddy Bay
Saint John
Bay of Fundy
Penobscot Bay
Bar Harbor
Grand Manan Basin
Digby
Halifax
Liverpool
Portland
Yarmouth
Emerald Basin
Jordan Basin
Nova Scotian Shelf
Portsmouth
Jeffrey's Ledge
SSW
Browns Bank
Cape Ann
Wilkinson Basin
Georges Basin
Boston
Cape Cod
annel
Georges Bank
Nantucket Shoals
Outflow
Great South Channel
Base map from USGS

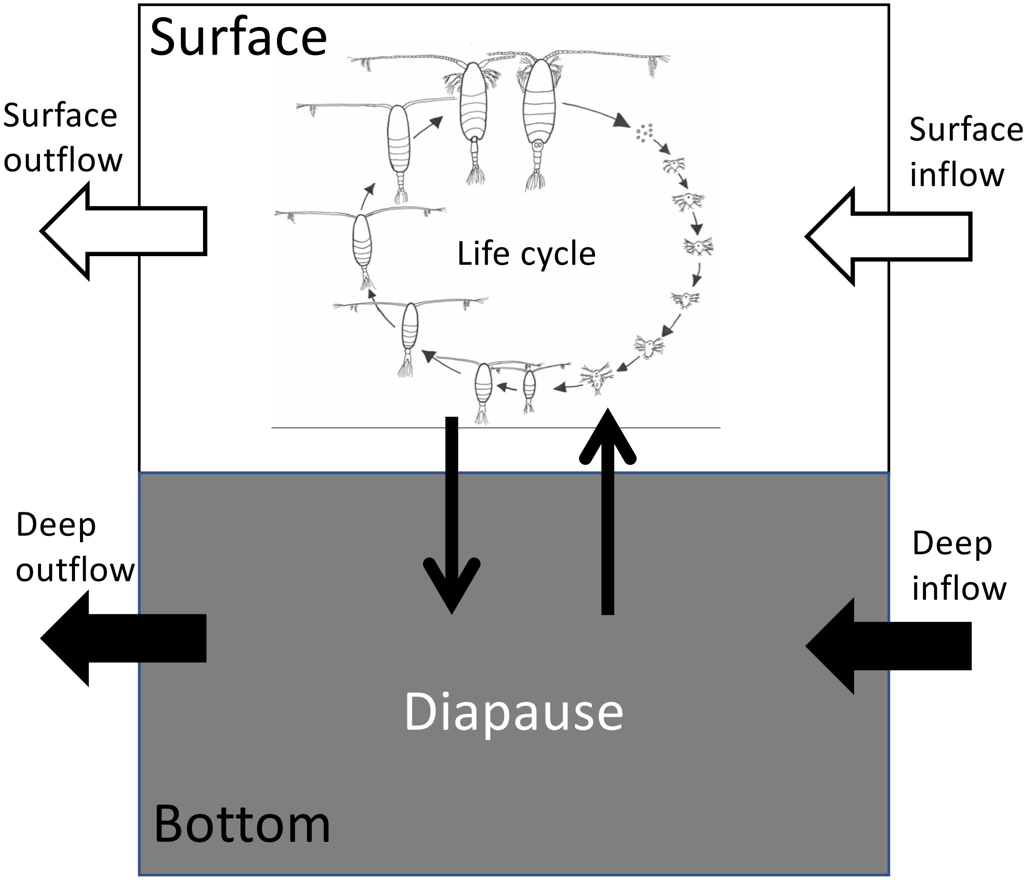
Surface
Surface outflow
Surface inflow
Life cycle
Deep outflow
Deep inflow
Diapause
Bottom

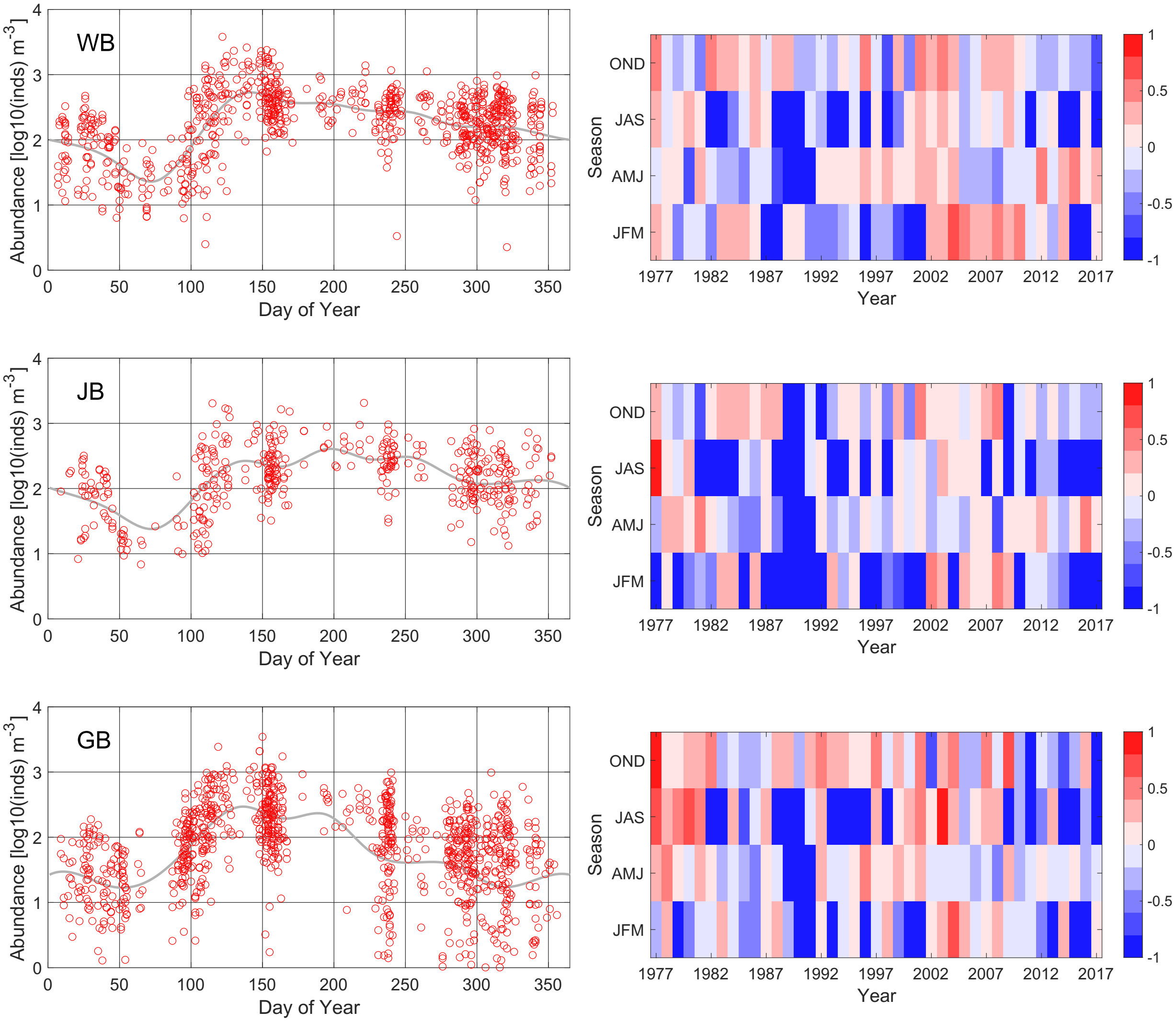
WB
JB
GB
Abundance [log10(inds) m^{-3}]
Day of Year
0
50
100
150
200
250
300
350
0
1
2
3
4
Season
OND
JAS
AMJ
JFM
Year
1977
1982
1987
1992
1997
2002
2007
2012
2017
1
0.5
0
-0.5
-1

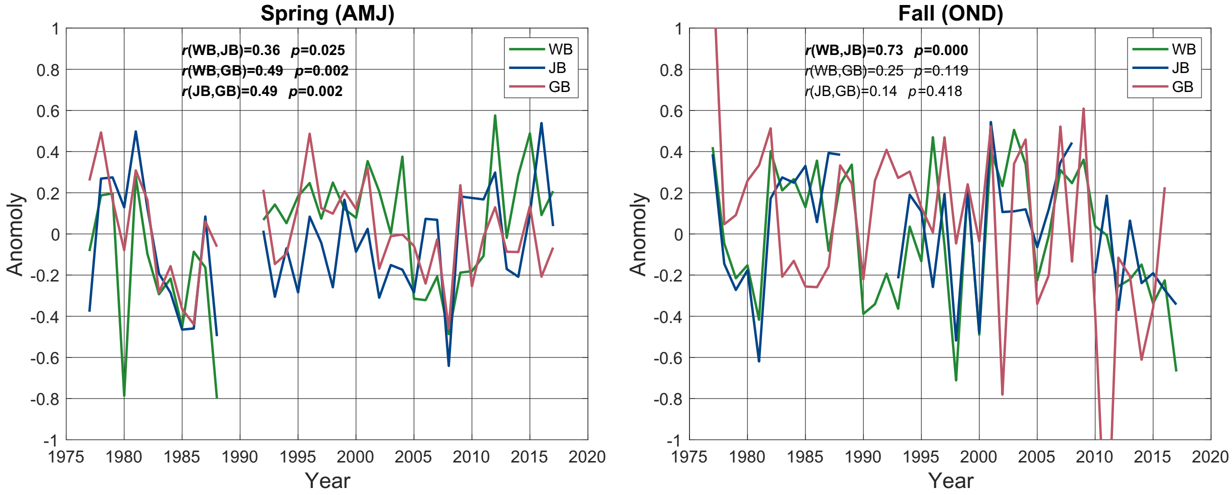
Spring (AMJ)
r(WB,JB)=0.36 p=0.025
r(WB,GB)=0.49 p=0.002
r(JB,GB)=0.49 p=0.002
WB
JB
GB
Anomoly
Year
1
0.8
0.6
0.4
0.2
0
-0.2
-0.4
-0.6
-0.8
-1
1975
1980
1985
1990
1995
2000
2005
2010
2015
2020
Fall (OND)
r(WB,JB)=0.73 p=0.000
r(WB,GB)=0.25 p=0.119
r(JB,GB)=0.14 p=0.418
WB
JB
GB
Anomoly
Year

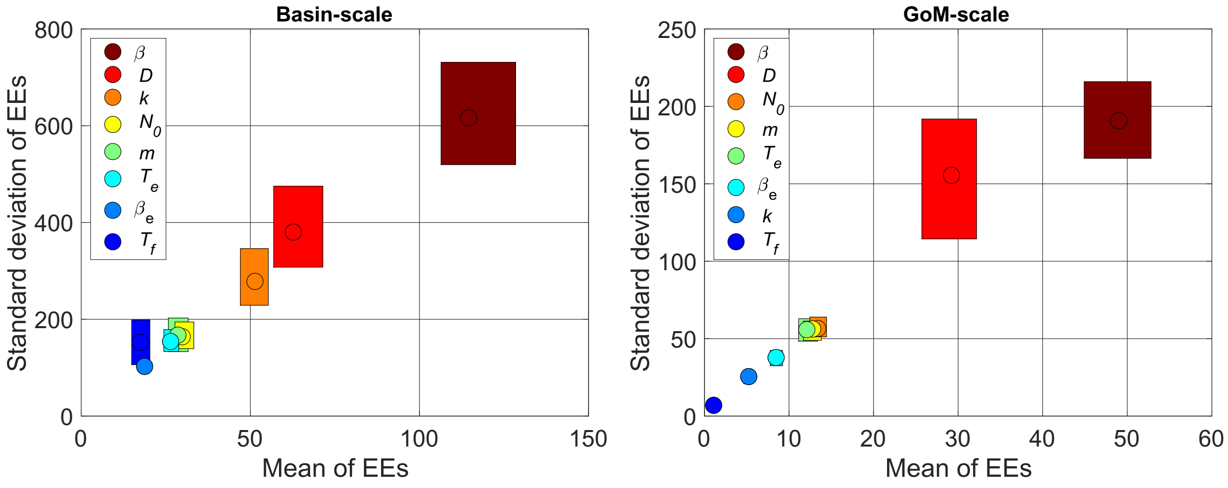
Basin-scale
Standard deviation of EEs
Mean of EEs
0
200
400
600
800
0
50
100
150
β
D
k
N0
m
Te
βe
Tf
GoM-scale
Standard deviation of EEs
Mean of EEs
0
50
100
150
200
250
0
10
20
30
40
50
60
β
D
N0
m
Te
βe
k
Tf

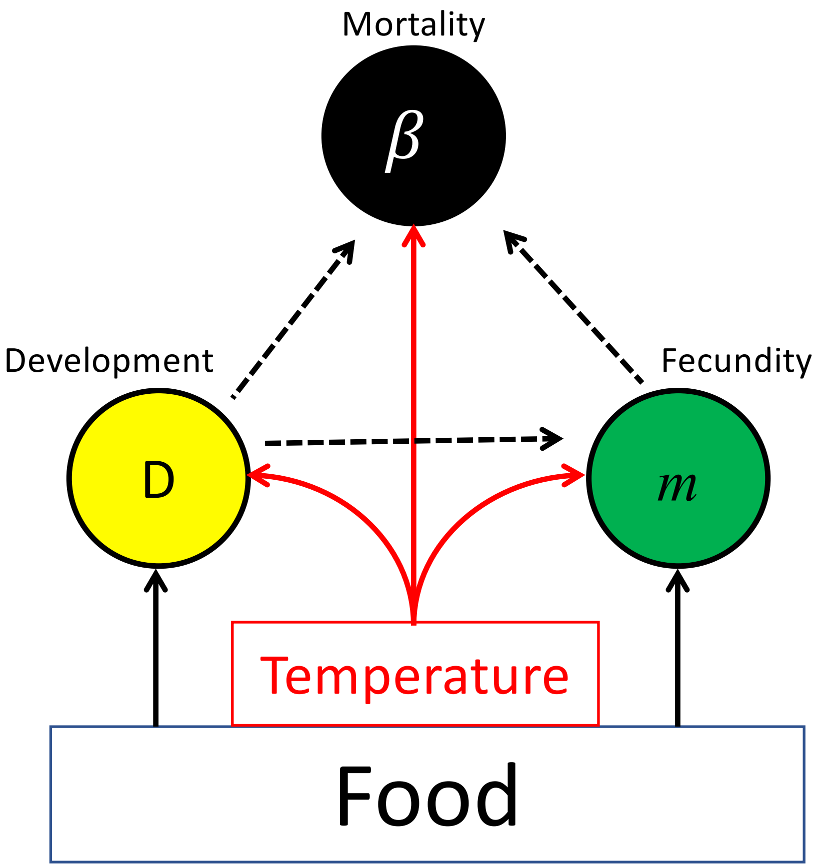
Mortality
β
Development
Fecundity
D
m
Temperature
Food

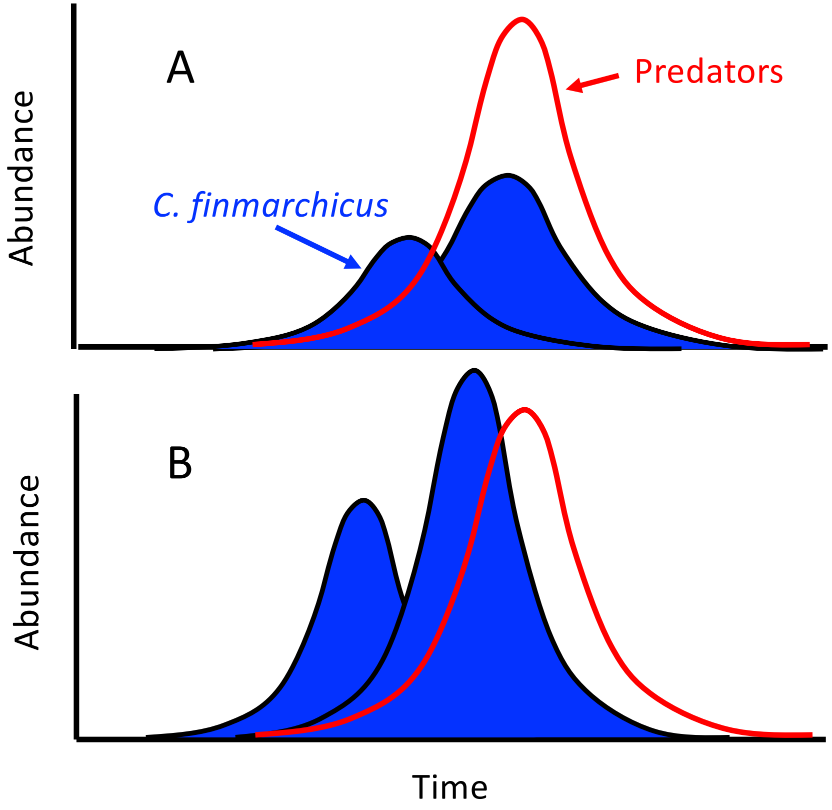
A
Predators
C. finmarchicus
Abundance
B
Abundance
Time